

## Anomalous kinetic energies of adsorbed $^4\text{He}$ on active carbon fibre (ACF)

This article has been downloaded from IOPscience. Please scroll down to see the full text article.

1999 J. Phys.: Condens. Matter 11 6653

(<http://iopscience.iop.org/0953-8984/11/35/303>)

View [the table of contents for this issue](#), or go to the [journal homepage](#) for more

Download details:

IP Address: 171.66.16.220

The article was downloaded on 15/05/2010 at 17:10

Please note that [terms and conditions apply](#).

## Anomalous kinetic energies of adsorbed $^4\text{He}$ on active carbon fibre (ACF)

D Nemirovsky<sup>†</sup>, R Moreh<sup>†</sup>, K H Andersen<sup>‡</sup> and J Mayers<sup>§</sup>

<sup>†</sup> Physics Department, Ben-Gurion University of the Negev, Beer-Sheva, Israel

<sup>‡</sup> Institut Laue–Langevin, BP 156, 38042 Grenoble Cédex 9, France

<sup>§</sup> Rutherford Appleton Laboratory, Chilton, Didcot, Oxon OX11 0QX, UK

Received 7 April 1999

**Abstract.** Direct measurements of the kinetic energies of He atoms adsorbed on active carbon fibre (ACF), at submonolayer coverage, are reported. The electronvolt spectrometer (eVs) of the ISIS neutron source, that utilizes the neutron Compton scattering technique, was employed. The specific adsorption area of the ACF was  $3000\text{ m}^2\text{ g}^{-1}$ . The momentum distribution of adsorbed helium was measured at 4.6 K and 10.2 K and the average kinetic energy  $K$ , was found:  $54.3 \pm 3.0\text{ K}$ . This value is 30% higher than that estimated by assuming slit-shaped pores of dimensions  $\sim 0.7\text{ nm}$  together with a nearly monolayer coverage on a graphitic type adsorber.

### 1. Introduction

The adsorption of helium on graphite in the form of Grafoil and other substrates has been investigated using many methods such as neutron diffraction and thermodynamic methods; the in-plane arrangement and phase transitions of this system has been studied in detail. The interaction potential between an He atom and a graphite surface, which has a well defined geometry, has also been investigated. The interaction was represented by a 6–12 Lennard-Jones potential which describes some of the properties of the system [1, 2]. In particular the out-of-plane potential has been calculated and the equilibrium distance of the He atoms above the graphite plane deduced. The specific heat of He monolayers on graphite, which form two-dimensional phases [3, 4] has also been studied. The corresponding Debye temperatures of the two-dimensional solid film of He were deduced and found to increase with coverage from 19 K to 58 K. More information about the two-dimensional He films adsorbed on graphite [5] was obtained by using neutron diffraction. The results of the above studies may be employed to estimate the zero-point kinetic energy of the adsorbed He atoms parallel to the graphite planes and also along the perpendicular direction, at coverages of around one monolayer.

In the present work, we studied the interaction between helium and the surface of active carbon fibre (ACF). In the nano-scale regime, the structure of the ACF resembles that of graphite (as discussed in more detail below); hence the interaction energy of He with the ACF is expected to be close in magnitude to that of He atoms enclosed between two graphite surfaces. The measurements were carried out using the neutron Compton scattering (NCS) technique [6, 7] where the momentum distribution of the He atoms adsorbed on an ACF surface has been obtained. The data yield the kinetic energies of adsorbed He atoms including the part arising from the zero-point motion. Submonolayer coverage of He on ACF was employed. This ensured that the main part of the interaction along the normal to the carbon surface is

between an He atom and the adsorber thus reducing the contribution of the He–He interaction along the same direction. In order to increase the ratio between the He signal and background, we selected an ACF with a huge surface area of  $\sim 3000 \text{ m}^2 \text{ g}^{-1}$ . In this connection, it should be emphasized that it is practically impossible to measure the kinetic energy of He adsorbed on graphite using the same method. This is because the specific surface area of Grafoil is  $\sim 25 \text{ m}^2 \text{ g}^{-1}$  only, hence the expected signal from He at a coverage of 1 ML adsorbed on 16.3 g of Grafoil (the same mass as that of the ACF used here) would be  $\sim 1\%$  of that obtained from the adsorbed He on ACF. Such a weak signal would be far below the detection limit of the eVs spectrometer at ISIS.

## 2. Experiment

The present experiment was carried out using the eVs spectrometer [6] of the ISIS neutron source at the Rutherford–Appleton Laboratory, UK. The incident n-beam is pulsed and has a continuum of energies in the range 1–100 eV. In the eVs instrument, one measures the time of flight (TOF) spectrum of the scattered neutrons from the sample to an array of neutron detectors alternately with and without a gold-foil absorber set in front of the n-detectors. The neutron absorption dip corresponds to the first resonance energy at 4912 meV in  $^{197}\text{Au}$ ; it defines the energy of the scattered neutron. The thickness of the gold foil absorber and the fact that Au has a single resonance in the energy region of interest ensures an adequate intensity and momentum resolution for scattering especially from low mass samples such as He. Two sets of TOF spectra were stored and accumulated in the computer memory every 5 min, corresponding to the gold foil absorbers placed in and out of the path of the neutrons reaching the n-detectors. A total beam charge of around  $2500 \mu\text{A h}$  protons on the spallation target was accumulated per TOF spectrum measured. Two detector banks were used, each containing eight Li-glass n-detectors, and were set at backward angles between  $125$  and  $150^\circ$  with respect to the direction of the incident neutron beam. These large scattering angles, in He, correspond to momentum transfers ranging from  $86$  to  $94 \text{ \AA}^{-1}$ . The detector angles were determined by replacing the adsorption sample by a powdered lead scatterer and measuring its well known neutron diffraction lines at thermal neutron energies. The data from the various detectors were summed up to increase the total statistics of the measurement, as discussed in section 3.

### 2.1. The ACF sample

The adsorbing cell consisted of a pure aluminum cylinder (36 mm diameter, 70 mm long) with 1 mm thick walls, in the region traversed by the neutron beam; it contained a 16.3 g adsorber of active carbon fibre (ACF3000, pitch based and obtained from Osaka Gas Corporation). The cell was mounted inside a variable temperature helium cryostat. The specific surface area of this type of ACF [8] is quoted to be  $\sim 3000 \text{ m}^2 \text{ g}^{-1}$ . This surface area is larger than the maximum theoretical limit (being  $2630 \text{ m}^2 \text{ g}^{-1}$ ) of a graphite sheet assumed to consist of a single graphene layer adsorbing on its two sides. In this connection it should be remarked that almost all activated carbons are non-graphitizable carbons characterized by ill defined crystalline micrographites. The *c*-spacing is slightly larger than that of graphite due to lack of alignment of the graphitic layers. Thus the maximum surface area which is valid in the case of pure graphitic surface is not expected to be true for ACF. In [9], the super-high specific surface area is explained by assuming the ACF as consisting of slit-shaped pores having three-walled graphitic sheets with sizes of around 8 nm. The modelling of the ACF pores as consisting of three-walled infinite graphitic sheets does not contradict the non-graphitizable nature of the

ACF. This is because the size of the *crystallites* of graphite are larger than 20 nm and the number of parallel sheets in each crystallite is far larger than that constituting the ACF. In addition, the actual distance between the graphitic layers in the ACF used in our calculations, 0.335 nm at 10 K, is larger than that of graphite, being 0.330 nm at 10 K. It turned out that this larger distance had no influence on the calculated He kinetic energies (see below).

The helium was transferred to the cell using a thin walled stainless steel tube (1.0 mm internal diameter). Prior to He insertion, the ACF was heated to 100 °C under vacuum at  $\sim 10^{-5}$  Torr for about 12 hours. Calibrated amounts of  $^4\text{He}$  were then transferred to the ACF cell placed inside the cryostat. A total of 16 litres of He gas (i.e.  $\sim 1$  litre of He/g of ACF), measured at ambient pressure and temperature, were inserted into the cell. The resulting He vapour pressure was 2.0 mbar at 4.6 K which increased to 430 mbar at 10.2 K. This amount of He corresponds to a coverage of  $\sim 0.8$  monolayer on the ACF. An identical aluminum cell containing 16.3 g of graphite powder and having a similar geometry to that other ACF was also used for background measurement. The incident and transmitted n-beam intensities were monitored using Li-glass scintillators. Most of the scattering was contributed by the carbon and the Al of the sample and was of the order of 8% of the incident beam intensity.

### 3. Results and discussion

#### 3.1. Measured kinetic energy of He on ACF

The TOF spectra of the He + ACF sample were taken at 4.6 K and 10.2 K, where the vapour pressures were 2.0 mbar and 430 mbar respectively. Background runs were also taken using the same cell but with no helium. A typical TOF spectrum taken at 10.2 K from one detector at backward angle is plotted in figure 1. The small separated line is that of He, while the strong intensity broad line arises from the combined contribution of carbon (of the ACF) and aluminum (of the walls of the cell).

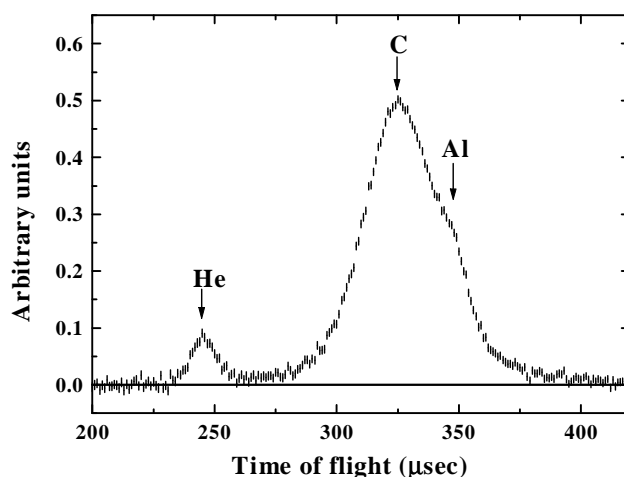


**Figure 1.** Time-of-flight spectrum of adsorbed helium on ACF (left peak) and that of the combined contribution of the aluminum container + carbon of the ACF (right peak). The spectrum (of a single detector) corresponds to a scattering angle  $142^\circ$ .

The data may also be displayed by defining a scaling function  $J(y)$  and using a scaling variable  $y$  related to the energy  $\omega$  and the momentum transfer  $q$  of the scattered neutron by:

$$y = (2\pi M/hq)(\omega - h^2q^2/8\pi^2M) \quad (1)$$

where  $M$  is the mass of the scatterer and  $h$  the Planck constant. Thus, the scaling function,  $J(y)$  may be written as:

$$J(y) = (2\pi\sigma_y^2)^{-1/2} \exp(-y^2/2\sigma_y^2) \quad (2)$$

with  $\sigma_y = (8\pi^2MK_s/3h^2)^{1/2}$  and  $K_s$  the *total* kinetic energy of the scattering atom; it is related to its effective temperature  $T_s$  (which include the part contributed by the zero-point motion of the He atom). It is given by:

$$K_s = 3kT_s/2 \quad (3)$$

where  $k$  is the Boltzmann constant. The data were summed over all detector angles in  $J(y)$  to increase the statistics. The results for He on ACF, after subtracting the spectrum of the same cell without He, are displayed in figure 2(a). A Gaussian line shape was fitted to the resulting experimental  $J(y)$  from which the variance  $\sigma_y$  of the Gaussian was derived. The value of  $\sigma_y$  represents the root-mean-square linear momentum along the  $y$  axis of the He atoms in units of  $\text{\AA}^{-1}$ . This yields the kinetic energy  $K_s$  of helium adsorbed on ACF at 4.6 K and 10.2 K (see table 1). In the particular case shown in figure 2(a), we obtained  $K_s = 58.1 \pm 6.3$  K for one bank of detectors. For the second bank, the result was  $K_s = 48.0 \pm 6.2$  K, yielding an average of  $K_s = 53.0 \pm 4.4$  K which is much higher than that of liquid He as discussed below. The measured  $K_s$  at 4.6 K, expected to be slightly lower than that at 10.2 K, is found to be higher; this is probably due to the increase in density of the He atoms because of cooling. In addition, since the measured kinetic energy is more than five times higher than the temperature of the measurement, the measured  $K_s$  is practically equal to the zero-point kinetic energy. Finally, the effect of neutron multiple scattering in the sample on the measured momentum distribution was calculated using a Monte Carlo program which accounted for sample geometry and for the instrumental resolution function. The resulting broadening effect of the multiple scattering on our measured value of  $K_s = 54.3 \pm 3.0$  K was less than 1 K. The final state effect (FSE) correction for deviations from the impulse approximation was performed using the method suggested by Sears [10].

**Table 1.** Weighted average kinetic energies  $K_s$  of He adsorbed on ACF and of liquid He on graphite deduced from the two banks of detectors. The temperatures at which the measurements were conducted are enclosed in parentheses. The average zero-point kinetic energy (denoted by an asterisk) was deduced from the values at 4.6 K and 10.2 K. The ‘calculated’ value was obtained by assuming an average ACF pore width of 0.8 nm with a standard deviation of 0.2 nm.

	He + ACF (4.6 K)	He + ACF (10.2 K)	He + ACF (average)	Calculated (K)	He + graphite (4.35 K)
$K_s$ (K)	$55.8 \pm 4.5$	$53.0 \pm 4.4$	$54.3^* \pm 3.0^*$	41.6	$16.5 \pm 2.7$

Similar TOF spectra were also measured at 4.35 K using an identical cell containing *powdered graphite* in which 16 litres of He at standard temperature and pressure were inserted. At 4.35 K, most of the He occurs in a liquid phase in this sample. The scattering from this last sample simulates the same experimental conditions as that of the He + ACF sample but is expected to yield nearly the same kinetic energy as that of liquid He at 4.35 K because graphite adsorbs only a very small amount of He. The same procedure discussed above was used for deducing  $K_s$  for this latter case. The measured  $J(y)$  plot for the He + graphite sample is given in figure 2(b). The measured value:  $K_s = (16.5 \pm 2.7)$  K (table 1) overlaps that reported in the

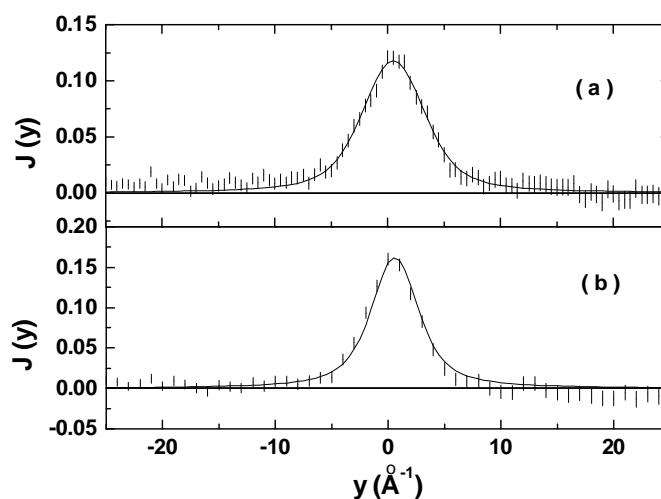


**Figure 2.** (a) Sum over eight  $J(y)$  spectra for He adsorbed on ACF at 10.2 K, for scattering angles between 125 and 150°. Solid lines represent the fitted  $J(y)$  function convoluted with the experimental resolution function obtained from a lead scatterer. The deduced kinetic energy for this bank of detectors is  $58.1 \pm 6.3$  K. (b) Sum over first 15  $J(y)$  spectra for the He + graphite sample, taken at 4.35 K. The deduced kinetic energy is  $16.5 \pm 2.7$  K.

literature [11, 12] for pure liquid He at 4.2 K. A small increment in  $K_s$  could, in principle, be contributed by the relatively small amount of the first few monolayers of adsorbed He ( $\sim 3\%$ ) on graphite that have a much higher kinetic energy.

### 3.2. Estimate of the kinetic energy of He on ACF

In order to obtain an estimate of the kinetic energy  $K_s$  of He adsorbed on ACF, we start by modelling the ACF as consisting of a system of graphitic slit-shaped pores, whose average width is taken to be 0.8 nm. This value is an average over the published pore sizes [9, 12–16] of different ACF types with large surface areas that were measured using He adsorption. These pore sizes were found to be smaller than those measured by nitrogen adsorption. Following [9], each slit is assumed to consist of an average of six infinite parallel graphitic planar sheets, three on each side of the slit atom as illustrated in figure 3. The thickness of each carbon sheet is taken to be  $d = 0.335$  nm. Here, the slit width is taken as the distance between the nuclei of carbon atoms on opposite walls of the slit enclosing the adsorbed He. Using this model, the problem of estimating  $K_s$  reduces to that of knowing the kinetic energy of He in two directions: along the normal to the graphitic planes of the slits and in a direction parallel to the planes of the slits. The kinetic energy  $K_n$  along the normal to the slits may be calculated by using the 6–12 Lennard-Jones pair potential describing the interaction between a single atom of a carbon plane and a single adsorbed He atom at a distance  $x$ ; it is given by [2]:

$$V(x) = 4\varepsilon[(\sigma/x)^{12} - (\sigma/x)^6] \quad (4)$$

where  $V$  has a minimum  $V = -\varepsilon$  at  $x = 2^{1/6}\sigma$  and  $V = 0$  at  $x = \sigma$ . By integrating the above potential over the two dimensions of the adsorbing graphite surface, the interaction between the graphite plane and an He atom, at a distance  $z$  from the plane of the C nuclei, is obtained:

$$V(z) = 2\pi\sigma^2\varepsilon\varphi[0.4(\sigma/z)^{10} - (\sigma/z)^4] \quad (5)$$

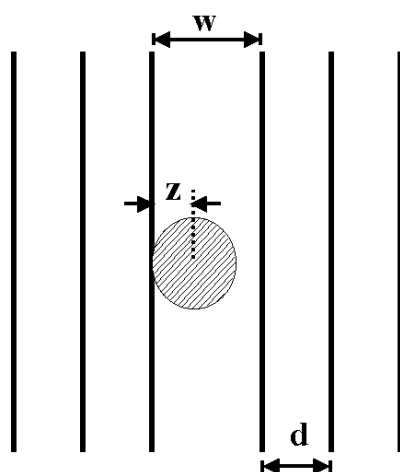


**Figure 3.** Schematic drawing showing an He atom enclosed within a slit-shaped pore consisting of three graphitic planes (represented by the solid lines) on each side of the atom. Each solid line passes through the C nuclei of the graphitic planes.

the parameters, taken from [2], are:  $\varepsilon = 1.40$  meV;  $\sigma = 2.74$  Å, is the distance from the surface at which  $V(z)$  is minimum;  $\varphi = 0.38$  Å<sup>-2</sup> is the atomic density of the C atoms in the adsorbing plane. The kinetic energy  $K_n$  of the He atoms *normal* to the planes of the *slit* was evaluated, at 0 K, by starting from equation (5) and using the Wentzel–Kramers–Brillouin (WKB) approximation. Here, we stick to the three-dimensional definition of the kinetic energy given in equation (3), namely:  $K_n = 3kT_n/2$  where  $T_n$  is the corresponding effective temperature along the normal to the graphitic planes.

The results were:  $K_n = 64.8$  K, 59.4 K and 67.2 K for three representative slit widths,  $w = 0.6$  nm, 0.8 nm and 1.0 nm respectively. It may be noted that the effect of varying the number of the graphitic walls on each side of the slit, between one and six, on the resulting value of  $K_n$  is quite small and is less than 1%.

An estimate of the kinetic energy  $K_p$  (at 0 K) *parallel* to the plane of the graphitic slit may be obtained from the specific heat results [3, 4] where the Debye temperature of the two-dimensional He film, at a coverage of 1 monolayer (ML), was reported to be:  $\theta_2 = 58$  K. This would imply that the two-dimensional zero-point kinetic energy of adsorbed He atoms at a coverage of  $\sim 1$  monolayer is  $K_p = \theta_2/2 = 29$  K. We used the value corresponding to 1 ML in spite of the fact that our coverage was  $\sim 0.8$  ML. The kinetic energy  $K_s$  of an He atom inside pores with uniform slit width  $w = 0.8$  nm is deduced by summing over the three components, one normal and two planar, yielding  $K_s = (2K_p + K_n)/3 = 39.1$  K which is  $\sim 30\%$  smaller than the measured value  $54.3 \pm 3.0$  K. It should be emphasized that if one accounts for the actual pore size distribution (PSD) of the ACF, the resulting kinetic energy of the He atoms remains essentially the same. This was tested by using the measured PSD reported, e.g. in [16] for a sample of pitched-based ACF having a specific surface area of  $795$  m<sup>2</sup> g<sup>-1</sup>, we obtained a kinetic energy of 40.6 K which is slightly higher than the above calculated value but much smaller than the measured one. All published types of ACF with any of the reported PSDs were found to yield the same  $K_s$  to within 4%. It is important to note that the above calculation yields an upper limit to the kinetic energy as it assumes that all He atoms are trapped between two surfaces and ignores the smaller kinetic energies of He atoms adsorbed on a single surface. Other He atoms which also reduce the calculated value are

those adsorbed on edges of the graphitic crystallites [9] where the surface density of C atoms is smaller, resulting in a lower He kinetic energies. From the above, it may be seen that the measured kinetic energy of the He atoms is anomalously larger than any value expected from the known widths of the slits of the ACFs. Finally, we calculated the slit width which would yield the measured He kinetic energy, 54.3 K, and obtained:  $w = 0.57$  nm. This slit width is much smaller than any of the experimental values spanning several types of ACF where the reported average widths [13–16] were between 0.75 nm and 1.4 nm and specific surface areas in the range 1000 to 2000  $\text{m}^2 \text{g}^{-1}$ .

The high kinetic energies may be explained by assuming that the ACF consists, in addition to the micropores accessible to  $\text{N}_2$ , of other ultramicropores with pore sizes between 0.50 nm and around 0.60 nm, so that the weighted averaged slit width of all pores is  $\sim 0.57$  nm. It may be noted in this connection that the ACF used in the present work contains ultramicropores which are accessible to He (but not to  $\text{N}_2$ ) and have a relatively large surface area exceeding that of the micropores by 50%. The slits widths of such ultramicropores must be smaller than  $0.34 + 0.29 = 0.63$  nm, where 0.34 nm is the thickness of a graphitic layer of ACF and 0.29 nm is the slit width which could accommodate a *flat*  $\text{N}_2$  molecule [17, 18]. The latter size was taken from n-diffraction measurements on graphite intercalated compounds such as  $\text{C}_{24}\text{K}$  and  $\text{C}_{24}\text{Rb}$  which are known to physisorb huge amounts of  $\text{N}_2$  at  $T < 200$  K inside the alkali planes [17, 18].

If the measured high kinetic energy is due solely to the occurrence of narrow slits in the ACF then this would indicate the occurrence of a confinement effect of He atoms in this type of ACF. However, such narrow slit widths in ACFs have not been reported yet. It may be argued that the large number of dangling bonds ( $\sim 10^{20}$  g) and some functional groups, such as carboxyl and carbonyl, occurring in commercial ACFs may enhance the He kinetic energies. This point was tested by repeating the same measurement by adsorbing neon gas on ACF, and no increase of the kinetic energy was observed. In addition, we found no theoretical treatment in the literature of the effect of dangling bonds and of the functional groups on He atoms.

The high kinetic energy may be explained by assuming that the ACFs have *cylindrical-shaped* pores of  $\sim 0.8$  nm diameter. There is no indication in the literature of the existence of such pores or nanotubes in the type of the ACF used in the present work.

It seems that the problem of He adsorption on ACF is intimately related to the adsorption of He on graphite and that the zero-point energies involved are strongly related to each other. The main input parameter is the size of the pores of the ACF adsorber. The main difficulty is that all measurements of the PSD in ACFs are model dependent involving uncertainties which are difficult to estimate.

#### 4. Conclusions

We have shown that the NCS technique may be used for measuring the He kinetic energies adsorbed on ACF. The measured values could be accounted for only by assuming that the ACF has an average slit widths of  $\sim 0.57$  nm. In evaluating the kinetic energy, we used the experimental He–graphite interaction in directions parallel to the graphitic planes of the ACF while the normal component was calculated using known Lennard-Jones potentials. Such narrow pores in active carbons were not reported in the literature. In this connection it is worth noting that all the known methods of deducing the pore sizes of the ACF are model dependent. It will be interesting to repeat the same measurement using other types of ACF with pores of different sizes. Finally, it should be remarked that a measurable amount of He is adsorbed on the ACF even at temperatures as high as 100 K. This would imply that the ACF used in the



present measurement contains ultra-micropores with sizes which allow He adsorption at such a high temperature.

### Acknowledgments

One of us (RM) would like to thank Professor K Kaneko from Chiba University and Professor T Enoki from Tokyo Institute of Technology for helpful discussions concerning the properties of the ACF and also for providing us with the ACF. Thanks are also due to Mr J Dreyer from the User Support Group at ISIS for his technical assistance in preparing the sample.

### References

- [1] Steele W A 1973 *Surf. Sci.* **36** 317
- [2] Carlos W E and Cole M W 1980 *Surf. Sci.* **91** 339
- [3] Bretz M, Huff G B and Dash J G 1972 *Phys. Rev. Lett.* **28** 729
- [4] Bretz M, Dash J G, Hickernell D C, McLean E E and Vilches O E 1973 *Phys. Rev. A* **8** 1589
- [5] Carneiro K, Passell L, Thomlinson W and Taub H 1981 *Phys. Rev. B* **24** 1170
- [6] Mayers J, Burke T M and Newport R J 1994 *J. Phys.: Condens. Matter* **6** 641
- [7] Rauh H and Watanabe N 1984 *Phys. Rev. Lett. A* **100** 244
- [8] Nakayama A, Suzuki K, Enoki T, Ishii C, Kaneko K, Endo M and Shindo N 1995 *Solid State Commun.* **93** 323
- [9] Kaneko K, Ishii C, Ruike M and Kuwabara H 1992 *Carbon* **30** 1075
- [10] Sears V F 1984 *Phys. Rev. B* **30** 44
- [11] Sosnick T R, Snow W M and Sokol P E 1990 *Phys. Rev. B* **41** 11 185
- [12] Mayers J, Andreani C and Colgnesi D 1997 *J. Phys.: Condens. Matter* **9** 10 639
- [13] Kaneko K, Setoyama N and Suzuki T 1994 *Studies Surf. Sci. Catal.* **87** 593
- [14] Economy J, Daley M, Hippo E J and Tandon D 1995 *Carbon* **33** 592
- [15] Ruike M, Kasu T, Setoyama N, Suzuki T and Kaneko K 1994 *J. Phys. Chem.* **98** 9594
- [16] Setoyama N, Ruike M, Kasu T, Suzuki T and Kaneko K 1993 *Langmuir* **9** 2612
- [17] Moreh R, Melloul S and Zabel H 1993 *Phys. Rev. B* **47** 10 754
- [18] Moreh R, Pinto H, Finkelstein Y, Volterra V, Birenbaum Y and Beguin F 1995 *Phys. Rev. B* **52** 5330